AGU PUBLICATIONS

Geophysical Research Letters

RESEARCH LETTER
10.1002/2015GL066795

Key Points:
- The fast response to cirrus cloud thinning is qualitatively opposite to that of CO_2 increase
- Cirrus cloud thinning avoids the weakening of the hydrological cycle in solar radiation management
- We present a methodologically simple way to carry out studies of cirrus cloud thinning

Supporting Information:
- Figures S14 and Table S1

Correspondence to:
J. E. Kristjánsson,
jegill@geo.uio.no

Citation:
Kristjánsson, J. E., H. Muri, and H. Schmidt (2015), The hydrological cycle response to cirrus cloud thinning, *Geophys. Res. Lett.*, *42*, 10,807–10,815, doi:10.1002/2015GL066795.

Received 29 OCT 2015
Accepted 21 NOV 2015
Accepted article online 25 NOV 2015
Published online 19 DEC 2015

The hydrological cycle response to cirrus cloud thinning

Jón Egill Kristjánsson[1], Helene Muri[1], and Hauke Schmidt[2]

[1]Department of Geosciences, University of Oslo, Oslo, Norway, [2]Max-Planck Institute of Meteorology, Hamburg, Germany

Abstract Recent multimodel studies have shown that if one attempts to cancel increasing CO_2 concentrations by reducing absorbed solar radiation, the hydrological cycle will weaken if global temperature is kept unchanged. Using a global climate model, we investigate the hydrological cycle response to "cirrus cloud thinning (CCT)," which is a proposed climate engineering technique that seeks to enhance outgoing longwave radiation. Investigations of the "fast response" in experiments with fixed sea surface temperatures reveal that CCT causes a significant enhancement of the latent heat flux and precipitation. This is due to enhanced radiative cooling of the troposphere, which is opposite to the effect of increased CO_2 concentrations. By combining CCT with CO_2 increase in multidecadal simulations with a slab ocean, we demonstrate a systematic enhancement of the hydrological cycle due to CCT. This leads to enhanced moisture availability in low-latitude land regions and a strengthening of the Indian monsoon.

1. Introduction

Due to slow progress in reducing anthropogenic greenhouse gas emissions and growing concern about the consequences of global warming, increasing attention is being paid to alternative ways of cooling down the climate [e.g., *Crutzen*, 2006; *Schäfer et al.*, 2015]. These so-called "climate engineering" (CE) or "geoengineering" techniques are often divided into two fundamentally different sets of approaches: greenhouse gas removal and solar radiation management (SRM). Cirrus cloud thinning is a form of radiation management (RM), which is different from SRM, because it is the longwave part of the electromagnetic spectrum that is targeted, as opposed to the shortwave.

Although global warming is often expressed in terms of temperature change, changes in the hydrological cycle are also of huge importance for society. There are indications that global warming is already causing disruptions to the hydrological cycle [*Syed et al.*, 2010], and climate projections indicate further drying of low- and middle-latitude land regions in the future [*Sherwood and Fu*, 2014], although globally, precipitation is expected to increase with increasing temperature. Can radiation management alleviate/avoid some of these problems, in addition to bringing down the global temperatures?

This question has recently been addressed in idealized multi-Earth System Model simulations (GeoMIP "G1" experiment) [see *Kravitz et al.*, 2011], in which the radiative forcing of an abrupt quadrupling of atmospheric carbon dioxide concentrations is counteracted by reductions in the solar constant [*Schmidt et al.*, 2012; *Kravitz et al.*, 2013a]. In these studies, even though the globally averaged temperature is restored, as there is no net radiative forcing, there is a systematic reduction in globally averaged precipitation by a few percent, which is a robust feature within the model ensemble [*Tilmes et al.*, 2013]. Associated with that, there is a reduction in moisture availability over land surfaces, as evidenced, e.g., by increased Bowen ratios [*Schmidt et al.*, 2012; *Kravitz et al.*, 2013b]. A qualitatively similar result was previously found in simulations by *Bala et al.* [2008], who canceled a doubling of CO_2 by reductions of the solar constant. *Kleidon et al.* [2015] recently proposed an analytical framework for addressing changes in the hydrological cycle from considerations of the surface energy budget.

Following up on the above studies, we pose the following question: Is the suppression of the hydrological cycle in these studies—even in the absence of any cooling of the climate—a general feature of radiation management, or can specific RM techniques avoid this suppression altogether? Some insight into these questions has been provided by simulations of desert brightening and marine cloud (or "marine sky") brightening. In the case of desert brightening, a negative radiative forcing is imposed only over land, and the result of that is a compensating secondary circulation, which further dries out land regions when compared to the nonengineered climate [*Bala and Nag*, 2011]. Conversely, in marine sky brightening, the negative radiative forcing

is only applied over ocean, and the resulting secondary circulation tends to enhance cloud formation and precipitation over low-latitude land regions [*Bala et al*., 2011; *Alterskjær et al*., 2013]. Likewise, in the case of stratospheric sulfur injections, *Haywood et al*. [2013] demonstrated a large sensitivity of Sahelian rainfall to interhemispherical differences in radiative forcing. *Niemeier et al*. [2013] compared the influence of different SRM techniques on the hydrological cycle and found systematic regional differences, even though for all studied techniques a reduction of the hydrological cycle was indicated.

The novelty of this study is that we investigate the response of the hydrological cycle to a largely unexplored CE idea, the so-called cirrus cloud thinning [*Mitchell and Finnegan*, 2009], which is fundamentally different from solar radiation management techniques in that it seeks to enhance the outgoing longwave radiation, rather than reducing the incoming solar radiation. This would be achieved by injecting a suitable number of efficient ice nuclei into regions of cirrus cloud formation, forcing a transition from homogeneous to heterogeneous freezing, leading to reduced cirrus optical depth [*Storelvmo et al*., 2013]. Targeting the longwave radiation is appealing in the sense that it is precisely the longwave part of the spectrum that is already being perturbed by increasing CO_2 concentrations. Therefore, since the suppression of the hydrological cycle is caused by incomplete cancelation of longwave and shortwave forcings [*Feichter et al*., 2004], this technique might conceivably avoid the suppression of the hydrological cycle discussed above.

The next section reviews the energetics of the hydrological cycle, linking atmospheric radiative cooling to surface fluxes of latent and sensible heat. This is followed by section 3 on the methodology applied, including experimental setup and diagnostics. We then present and interpret results from the model experiments (section 4), before the study is summarized and conclusions are drawn in section 5.

2. The Energetics of the Hydrological Cycle

As demonstrated and explained by, e.g., *Mitchell et al*. [1987], *Allen and Ingram* [2002], and *Held and Soden* [2006], the strength of the hydrological cycle is not determined so much by the availability of moisture as by the availability of energy. In a stationary climate, the troposphere is in energy balance, the main components of which are a radiative cooling due to greenhouse gases (H_2O, CO_2, etc.) and clouds, compensated by turbulent fluxes of latent heat (LH) and—to a lesser extent—(a) sensible heat (SH) from the Earth's surface and (b) radiative warming due to absorption of solar radiation by mainly H_2O. The latent heat flux provides the atmosphere with the water vapor that enables precipitation, and its magnitude is thus an indicator of the strength of the hydrological cycle. As the climate warms, the radiative cooling of the troposphere increases (mainly because of a higher emission temperature), and therefore, the latent heat flux will increase to restore the energy balance, leading to an increase in precipitation. However, the degree to which the precipitation increases with increasing temperature depends significantly on the cause of the warming. If, as is currently the case, the warming is caused by increased CO_2 concentrations, then the precipitation increase of about 2–3%/K [*Allen and Ingram*, 2002; *Held and Soden*, 2006] will be significantly less than what might be expected from, e.g., the Clausius-Clapeyron relationship, which would indicate a 7% increase per degree Kelvin [*Wu et al*., 2010]. This is partly because the CO_2 increase, when viewed in isolation from the temperature change, causes a reduction in the longwave cooling of the troposphere, because the radiative flux divergence is reduced [*Allen and Ingram*, 2002], and the rate of radiative cooling is proportional to it.

This result has many implications, one of them being that climate engineering in the form of solar radiation management cannot simultaneously restore both globally averaged temperature and precipitation to preindustrial (or equivalent) values [*Bala et al*., 2008; *Irvine et al*., 2010]. Multimodel studies with Earth System Models have confirmed that result [*Kravitz et al*., 2013a; *Tilmes et al*., 2013], e.g., when running the GeoMIP G1 experiment, as explained in section 1.

3. Methodology

In this section, we describe the numerical simulations that were carried out to investigate the influence of cirrus cloud thinning (CCT) on the hydrological cycle, as well as some of the diagnostics. The model tool is the Norwegian Earth System Model (hereafter NorESM), described in detail by *Bentsen et al*. [2013]. The atmospheric component is based on the National Center for Atmospheric Research CCSM4 (Community Climate System Model version 4), but with its own aerosol module [*Kirkevåg et al*., 2013]. The ocean component in

NorESM is a modified version of the Miami Isopycnic Coordinate Ocean Model [*Bleck et al*., 1992], but in this study, we instead use CCSM4's slab ocean model [*Neale et al*., 2010] along with its sea ice model (CICE4) and the Community Land Model 4 [*Oleson et al*., 2010; *Lawrence et al*., 2011].

3.1. Experimental Setup

In NorESM, cloud formation takes place whenever the relative humidity exceeds a threshold value (of about 80–90% depending on cloud type) [*Neale et al*., 2010], and cloud condensation nuclei are activated [*Hoose et al*., 2009]. Clouds forming at temperatures (T) below the homogeneous freezing threshold of 238 K are here termed "cirrus clouds," and CCT is only performed for such clouds. Similarly to *Muri et al*. [2014], cirrus cloud thinning is simulated by artificially enhancing the fall speeds of ice crystals in the atmosphere. This avoids the computationally demanding calculations of the competition between homogeneous and heterogeneous freezing from theoretical approaches, as was done by *Storelvmo et al*. [2013, 2014] and *Storelvmo and Herger* [2014]. The advantage is that many models may be able to carry out CCT simulations, which is now being planned in GeoMIP [*Kravitz et al*., 2015]. Support for using ice crystal fall speed enhancements as a proxy for CCT is found by noting the similarity in cloud cover changes between the fall speed experiments [*Muri et al*., 2014, Figure 2a] and the more complex experiments [*Storelvmo et al*., 2013, Figure 3d]. A major novelty here is that we have carried out simulations in which cirrus cloud thinning is done simultaneously to a CO_2 doubling. This enables us to directly address the competing influences of greenhouse gases and high clouds on the hydrological cycle. As in *Muri et al*. [2014], to get more confidence in our assessment of how cirrus cloud thinning influences climate, we have also carried out sensitivity runs, in which the cirrus clouds are made denser rather than thinner by reducing the ice crystal fall speeds. This can be viewed as an analogy to the "overseeding" case in *Storelvmo et al*. [2013].

Results from the following eight NorESM simulations will be presented below: (1) *ref*: preindustrial reference (control) simulation; (2) *thin2*: ice crystal fall speeds doubled at $T < 238$ K, otherwise unchanged; (3) *thin8*: ice crystal fall speeds increased eightfold at $T < 238$ K, otherwise unchanged; (4) *thick2*: ice crystal fall speeds divided by 2 at $T < 238$ K, otherwise unchanged; (5) *thick8*: ice crystal fall speeds divided by 8 at $T < 238$ K, otherwise unchanged; (6) *2xCO2*: CO_2 concentrations doubled; (7) *thin8+2xCO2*: a combination of experiments (3) and (6) yielding approximately zero net radiative forcing; and (8) *thin2+1.5xCO2*: a combination of experiment (2) and a CO_2 increase, yielding approximately zero net radiative forcing. Following *Bala et al*. [2010], each simulation was run in two setups: (a) 30 year runs with fixed sea surface temperatures (SSTs) and (b) 50 year runs with a slab ocean. The fixed-SST runs were carried out to enable quantification of the fast response to cirrus cloud thinning, while the slab ocean runs enable us to capture the time evolution of the full climate response (fast + slow). In one of the slab ocean experiments, *thin8*, an unphysical bifurcation into a "snowball-Earth" type of climate took place, due to an interaction between persistent, dense low clouds off the coast of Peru and strong radiative cooling of the underlying ocean. Such behavior, which is not uncommon in slab ocean configurations, is related to the lack of vertical mixing in the mixed-layer ocean and does therefore not happen in a fully coupled model configuration. Because of this problem, in Figures 2e and 3e below we approximate the climate effect from *thin8* by taking the difference between the *thin8+2xCO2* and *2xCO2* simulations.

3.2. Diagnostics

In order to extract the fast response of the hydrological cycle to CCT, we consider the radiative flux divergence for the atmosphere, which is linked to latent heat release through the following relation (neglecting stratospheric adjustment):

$$\Delta \mathrm{LH} + \Delta \mathrm{SH} \approx \Delta F^{\downarrow}_{\mathrm{surface}} - \Delta F^{\uparrow}_{\mathrm{surface}} - \left(\Delta F^{\downarrow}_{\mathrm{TOA}} - \Delta F^{\uparrow}_{\mathrm{TOA}}\right) + \Delta \dot{Q} \tag{1}$$

where Δ denotes changes relative to the control run, each of the radiative flux (F) terms represents the sum of solar and terrestrial radiation, and $\dot{Q}$ expresses the rate of change in the atmosphere's heat content [*Trenberth et al*., 2001], which can be approximated as $\dot{Q} = \frac{p_s}{g}\left(c_p \frac{\mathrm{d}\overline{T}}{\mathrm{d}t} + L\frac{\mathrm{d}\overline{q}}{\mathrm{d}t} + \frac{\mathrm{d}\overline{k}}{\mathrm{d}t} + \frac{\mathrm{d}\overline{\Phi}}{\mathrm{d}t}\right)$, $\overline{T}$ being the vertically and horizontally averaged temperature of the atmosphere, $\overline{q}$, $\overline{k}$, and $\overline{\Phi}$ the corresponding averages for specific humidity, kinetic energy, and potential energy, respectively, c_p is the specific heat capacity at constant pressure, L the latent heat of condensation, g gravity, and p_s the globally averaged surface pressure.

Table 1. Global Annual Averages of Selected Quantities From Fixed-SST Simulations[a]

	thin8 Minus *ref*	*thick8* Minus *ref*	*2xCO2* Minus *ref*	*thin8+2xCO2* Minus *ref*	*thin2+1.5xCO2* Minus *ref*
RFDIV ($W m^{-2}$)	+5.69 ± 0.22	−4.63 ± 0.20	−1.73 ± 0.19	+3.91 ± 0.20	+1.50 ± 0.21
LH ($W m^{-2}$)	+4.65 ± 0.24	−3.82 ± 0.26	−2.03 ± 0.25	+2.63 ± 0.28	+0.92 ± 0.25
Precipitation ($mm d^{-1}$)	+0.161 ± 0.008	−0.132 ± 0.009	−0.070 ± 0.008	+0.091 ± 0.009	+0.032 ± 0.009
T_s (K)	−0.30 ± 0.051	+0.30 ± 0.046	+0.27 ± 0.047	−0.021 ± 0.046	+0.016 ± 0.047
RTOA ($W m^{-2}$)	−3.4 ± 0.35	+3.5 ± 0.25	+3.4 ± 0.29	+0.11 ± 0.39	+0.22 ± 0.31

[a]The values express differences from the control run (ref). RFDIV (radiative flux divergence) is the sum of the four "ΔF" terms in equation (1); LH is latent heat flux from the surface, precipitation is total precipitation (stratiform + convective), T_s is near-surface temperature, while RTOA represents the net downward flux at the top of the atmosphere. The values after ± represent one standard deviation, based on the 30 annual means.

To assess the influence of the changes in the hydrological cycle on water availability over land, we consider the difference between precipitation and potential evapotranspiration (PET) [*McVicar et al.*, 2005, equation (2.18)]. PET is the evapotranspiration that would take place in the case of unlimited water availability from the surface. A negative value of "*P* minus PET" is indicative of dry soil conditions, and some studies have defined various thresholds of the ratio *P*/PET to indicate different degrees of dryness [e.g., *Feng and Fu*, 2013]. We prefer *P* minus PET to *P* minus *E* (*E* being evapotranspiration), as the latter tends to zero under dry conditions and is therefore less informative than *P* minus PET.

4. Results

4.1. The Global Hydrological Cycle

We now turn our attention to the hydrological cycle, and as explained in section 3.2, we start by looking at the atmospheric radiative flux divergence in the fixed-SST runs (Table 1 (top row) and supporting information Figure S1). Globally averaged we notice that CCT (*thin8 minus ref*) is associated with a substantial increase in the radiative flux divergence, which, as expected from equation (1), results in an increase in latent heat flux (Table 1). There is a corresponding increase in globally averaged precipitation (Table 1), despite the fact that the climate is experiencing a slight cooling (Table 1), which inevitably would tend to dampen the hydrological cycle. Cirrus cloud thickening (*thick8* minus *ref*) has the opposite effect (Table 1 and Figure S1b), and we find a globally averaged reduction of the radiative flux divergence, with an associated suppression of the latent heat flux. In this case, the globally averaged precipitation is reduced despite a slight warming. We note that even though the surface temperature change is of the same magnitude but with opposite sign in *thin8* compared to *thick8*, the precipitation change is almost 20% larger in *thin8*. This nonlinearity is probably sensitive to the amount and optical thickness of cirrus clouds in the control climate, and we defer further investigation of that to future studies. Doubling of CO_2 would by itself (*2xCO2* minus *ref*) weaken the hydrological cycle, as discussed in section 2 and indicated by reduced radiative flux divergence in Table 1 and Figure S1c. When cirrus cloud thinning and CO_2 doubling are combined (Table 1 and Figure S1d), we note that even though the globally averaged temperature change is almost zero, there is an enhancement of the hydrological cycle.

Further insight into the response of the hydrological cycle to cirrus cloud thinning is obtained by investigating the time evolution of surface temperature and latent heat flux from the surface in the slab ocean experiments (Figure 1). The red dots give the results from CO_2 doubling, which are very similar to Figure 2 in *Allen and Ingram* [2002], showing that even for an ~1 K warming, there is no increase in the latent heat flux. The green dots are from the combined CO_2 doubling and cirrus cloud thinning experiment. As the two effects almost cancel each other in terms of radiative forcing, there is virtually no drift; therefore, the points—apart from some scatter—clump around a slight residual warming of about 0.2 K and a substantial increase in latent heat flux of about 3 $W m^{-2}$ (Table S1). This confirms the indication from Table 1 that for the eightfold increase of ice crystal fall speeds in cirrus clouds, there is a significant enhancement of the hydrological cycle, even in the absence of global warming (viz., *y* axis intercept of dots in Figure 1). The dark blue dots show the corresponding result for cirrus cloud thickening alone. We note that the fit line is approximately parallel to the one for CO_2 doubling, but shifted to the right, indicating that in the fast response there is an even stronger suppression of the hydrological cycle from our cirrus cloud thickening than from CO_2 doubling. As seen in Figure 1, the results of the

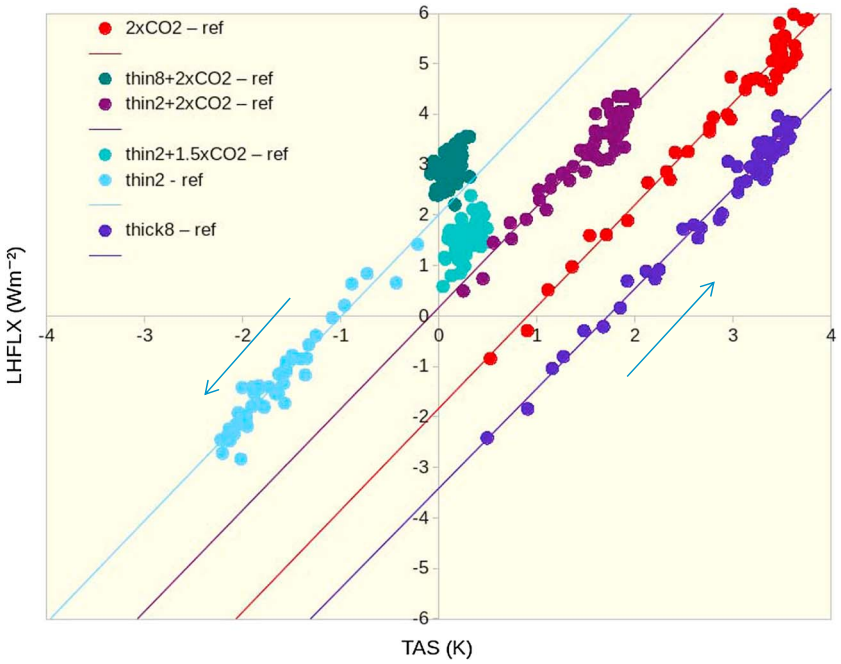

Figure 1. A scatterplot—based on NorESM1-M slab ocean runs—of global annual mean difference in surface air temperatures (*x* axis; in K) versus change in latent heat flux (*y* axis; in W m^{-2}) where each dot represents one model year between experiments (from right to left in the figure): *thick8* minus *ref* (blue), *2xCO2* minus *ref* (red), *thin2+2xCO2* minus *ref* (purple), *thin2+1.5xCO2* minus *ref* (turquoise), *thin8+2xCO2* minus *ref* (green), and *thin2* minus *ref* (light blue). The time evolution is indicated by the direction of the arrows. For two of the runs (*thin2+1.5xCO2* minus *ref* and *thin8+2xCO2* minus *ref*) the points cluster with no clear time evolution due to near-zero net radiative forcing.

experiments with more moderate changes in cirrus properties or CO_2 concentration, given by light blue dots (*thin2* minus *ref*), purple (*thin2 plus 2xCO2* minus *ref*), and turquoise (*thin2 plus 1.5xCO2* minus *ref*), are in full qualitative agreement with the results from the other experiments.

In the *thin8+2xCO2* simulation, there is a slight reduction in total atmospheric water vapor (supporting information Table S1) due to cooling in the tropics (supporting information Figure S2a), which is not present in *thin2+1.5xCO2* (supporting information Figure S2b). This will be further explored in upcoming studies.

4.2. Precipitation Response Patterns

Having established a strengthening of the hydrological cycle through cirrus cloud thinning, we now investigate how this is manifested in terms of precipitation patterns. Several previous studies have highlighted possible detrimental effects of solar radiation management on the Indian monsoon [e.g., *Robock et al.*, 2008; *Tilmes et al.*, 2013], and we pay particular attention to this feature. Figure 2 shows the June-July-August-September precipitation anomalies relative to the reference run, while annual averages are shown in supporting information Figure S3. First, in Figures 2a and 2b we show the results of cirrus cloud thinning on top of CO_2 doubling in two model simulations. In both cases, despite the absence of global warming (cf. columns 4 and 5 of Table 1), we see statistically significant increases in precipitation in many regions. This includes, e.g., the Sahelian region, as well as the Indian subcontinent. For comparison, we show in Figures 2c and 2d the precipitation changes in two global warming experiments, i.e., CO_2 doubling and cirrus cloud thickening, respectively (cf. columns 2 and 3 in Table 1). As expected in a warmer climate, there is a significant overall increase in precipitation, but we also see certain land regions (e.g., northern South America) with very large reductions in precipitation. To separate the different contributions from CCT and CO_2 doubling, we in Figure 2e show the effect of CCT alone. Here even though the climate is colder than the reference climate (cf. column 1 in Table 1), there are several low-latitude regions with statistically significant increases in precipitation. Importantly, this includes both the Indian monsoon region and the Sahel.

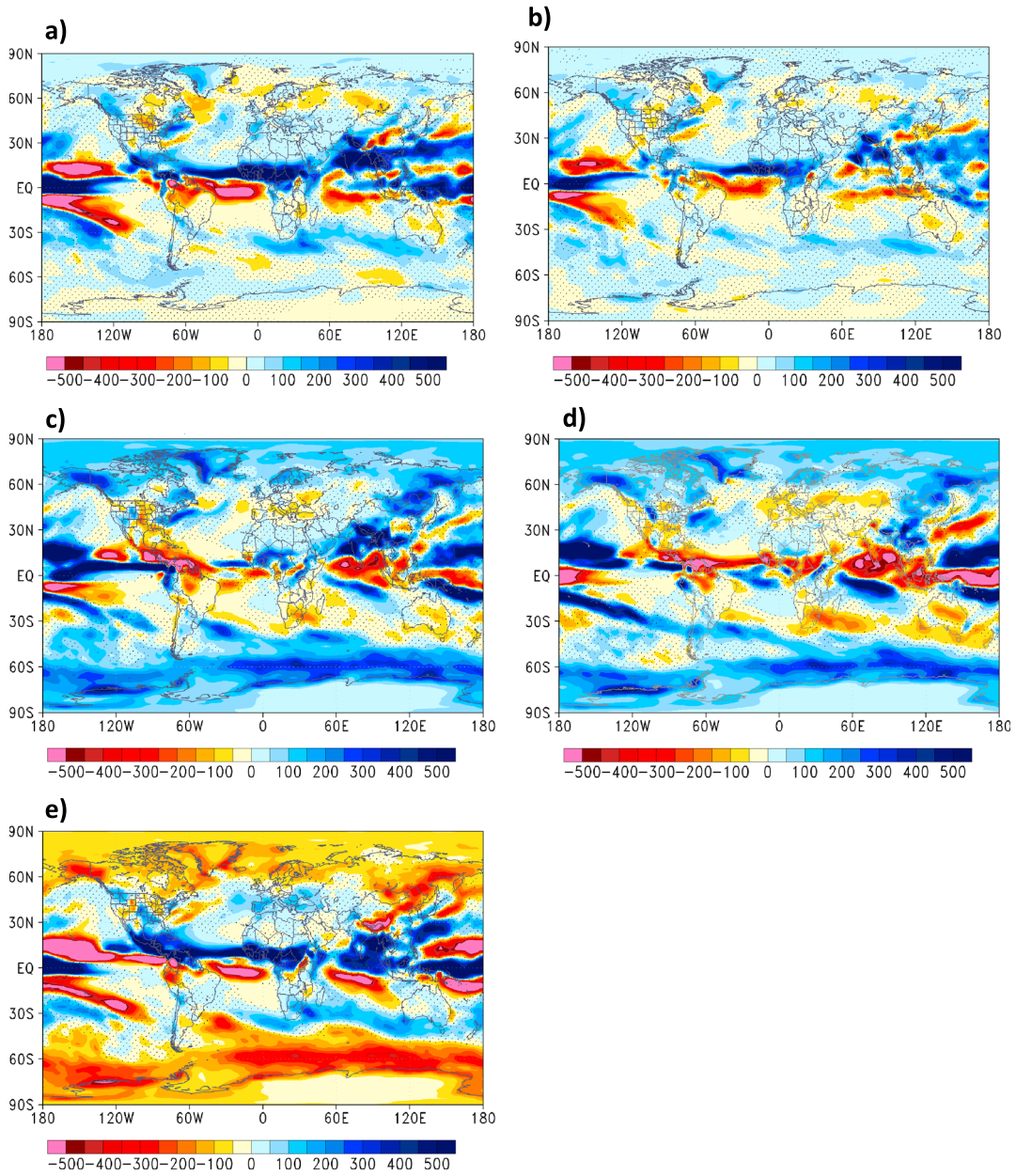

Figure 2. June-July-August-September (JJAS) mean precipitation difference, averaged over the last 30 years (out of 50) of the slab ocean runs. Nonstippling indicates a level of confidence higher than 90%. Units: mm yr^{-1}. (a) *thin8+2xCO2* minus *ref*, (b) *thin2+1.5xCO2* minus *ref*, (c) *2xCO2* minus *ref*, (d) *thick8* minus *ref*, and (e) *thin8+2xCO2* minus *2xCO2*.

4.3. Moisture Availability Over Land Regions

Changes in precipitation alone are not necessarily a good indicator for, e.g., impacts on agriculture, where moisture availability may be more relevant. A powerful measure of this, as mentioned in section 1, is the quantity *P* minus PET, displayed in Figures 3a–3e for the same experiments as in Figure 2. Again, we focus on the June-July-August-September season while annual averages are shown in supporting information Figure S4. Starting with combined CCT and CO_2 doubling (Figures 3a and 3b), we find significant enhancements of soil moisture availability over many low-latitude land regions, especially Africa between 0°N and 20°N, the Indian subcontinent, Indochina, and much of Indonesia. On the other hand, northeastern South America, parts of China and NE Europe show a decrease. These changes are particularly pronounced in the stronger CCT and CO_2 forcing case (Figure 3a), whereas they are weaker but with similar spatial patterns in the weaker forcing scenario (Figure 3b).

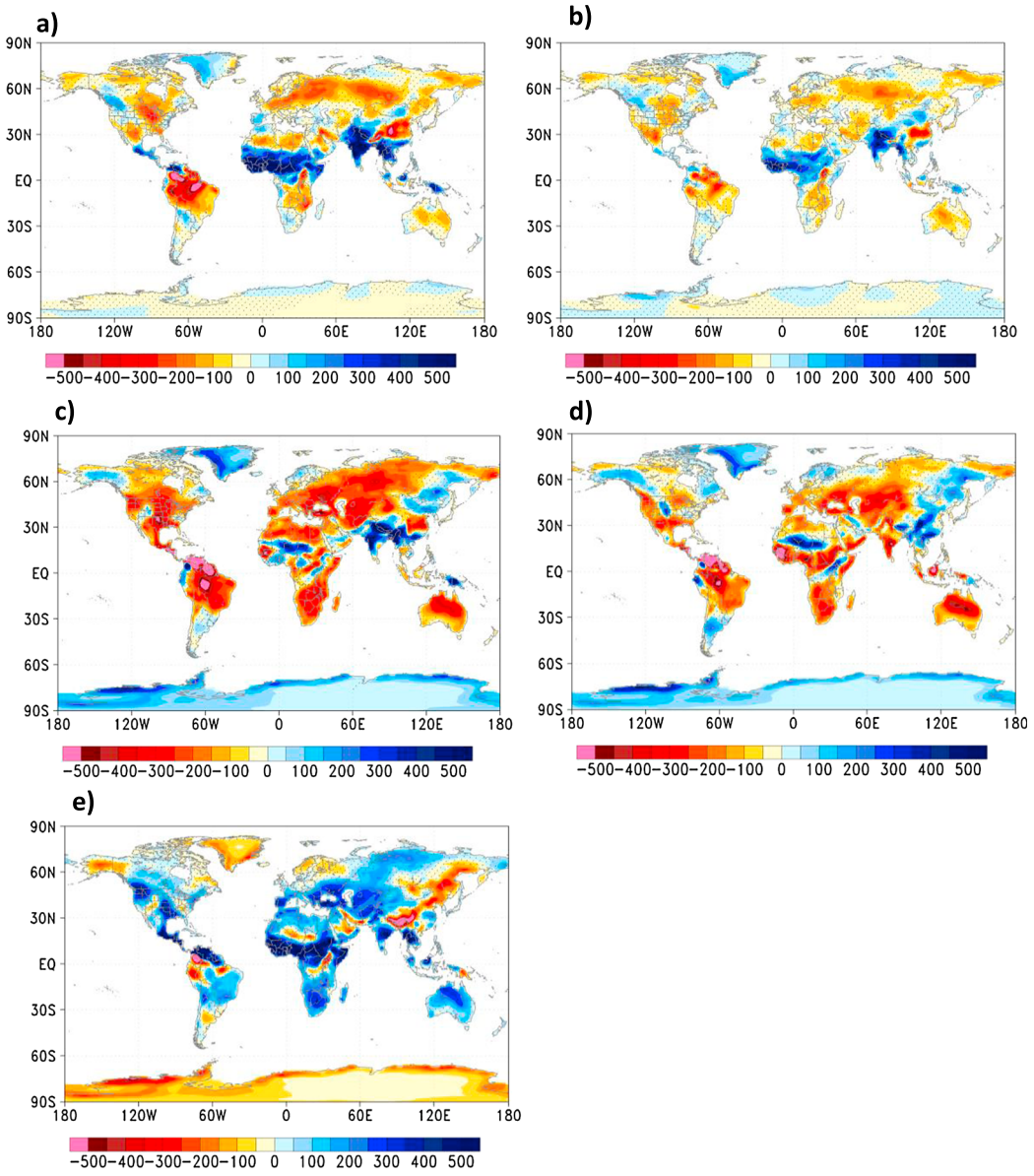

Figure 3. JJAS mean difference in precipitation minus potential evapotranspiration (*P* minus PET), averaged over the last 30 years (out of 50) of the slab ocean runs. Nonstippling indicates a level of confidence higher than 90%. Units: mm yr^{-1}. (a) *thin8+2xCO2* minus *ref*, (b) *thin2+1.5xCO2* minus *ref*, (c) *2xCO2* minus *ref*, (d) *thick8* minus *ref*, and (e) *thin8+2xCO2* minus *2xCO2*. Note that only values over land are shown.

The pure CO_2 doubling and cirrus cloud thickening experiments show a dramatic drying trend over many land regions (Figures 3c and 3d), especially at low latitudes, in particular in northern South America, the Sahel region, and Australia, while also central Asia and western parts of the United States and Europe now have statistically significant reductions in soil moisture availability. These reductions are consistent with simulated changes in soil moisture reported by CMIP5 models for the end of the 21st century [e.g., *Collins et al.*, 2013, Figure 12.23]. Comparing to the precipitation signal alone in Figures 2c and 2d, we note a huge difference, highlighting the usefulness of potential evapotranspiration as an indicator of increasing evaporative demand in a warming climate. Comparing Figures 3a and 3b to Figures 2a and 2b, we see smaller differences, because there is virtually no global warming in these experiments and therefore the evaporative demand changes less. This result is confirmed by Figure 3e, which gives the effect of CCT alone, showing increased moisture availability in most regions, especially Sahel, Central America, India, and Indochina, but with reductions extending northeastward from Himalaya.

5. Summary and Conclusions

Through a series of Earth System Model simulations we have investigated the response of the hydrological cycle to climate engineering in the form of cirrus cloud thinning. By separating fast responses in fixed-SST simulations from slow responses from multidecadal slab ocean simulations, we are able to get a clear physical picture of the link between the hydrological cycle and the atmospheric energetics that constrain it [e.g., *Allen and Ingram*, 2002; *Held and Soden*, 2006]. We find that the fast response is characterized by an enhanced atmospheric radiative cooling and an associated increase in the release of latent heat and thereby precipitation. Hence, when cirrus cloud thinning is combined with CO_2 increase in such a way that the net radiative forcing is almost zero, there is a significant net increase in latent heat release and precipitation. As a result of these changes, we find clear evidence of a strengthening of Sahelian rainfall and the Indian monsoon in simulations with combined CCT and CO_2 increase. Simulations with the opposite of cirrus cloud thinning, i.e., "cirrus cloud thickening" give in almost every aspect, qualitatively, the opposite results, i.e., a weaker hydrological cycle in the fixed-SST simulations, exhibiting a behavior similar to that of CO_2 doubling alone.

The opposite impacts of CO_2 doubling and CCT on the hydrological cycle become very clear when we investigate changes in soil moisture availability over land regions, as measured by P minus PET: While CCT alone leads to increased moisture availability in most land regions, especially at low latitudes, the opposite is found for CO_2 doubling, with particularly detrimental effects over northern South America.

We conclude that cirrus cloud thinning inherently leads to an enhancement of the hydrological cycle and that it therefore has the potential to avoid the suppression of precipitation found in earlier multimodel studies with solar radiation management. We have introduced a methodologically simple way to carry out studies of cirrus cloud thinning that avoids the complicated physics involved (competition between homogeneous and heterogeneous freezing), and it is our hope that this will stimulate a follow-up of this study by many Earth System Models. This is important, because in particular, the regional aspects of our results are likely to be model dependent. All our model simulations make the naïve assumption that climate engineering in the form of cirrus cloud thinning is feasible, but in reality, very little is known about the feasibility of cirrus cloud thinning at this point and the technological challenges that it might entail.

Acknowledgments

The work by J.E.K. and H.M. was supported by the EXPECT project, grant 229760/E10, funded by the Norwegian Research Council. In addition, J.E.K. and H.M. were supported by the Norwegian Research Council's Supercomputing Programme (NOTUR) through a grant of computing time. J.E.K. benefited from stimulating discussions with various colleagues during sabbatical stays at the Max-Planck Institute for Meteorology in Hamburg and the National Center for Atmospheric Research in Boulder in 2014. The work of H.S. was supported by the German Science Foundation (DFG) within projects CEIBRAL and ComparCE. The data from the model simulations are available from the authors upon request.

References

Allen, M. R., and W. J. Ingram (2002), Constraints on future changes in climate and the hydrologic cycle, *Nature*, *419*, 224–232.

Alterskjær, K., J. E. Kristjánsson, O. Boucher, H. Muri, U. Niemeier, H. Schmidt, M. Schulz, and C. Timmreck (2013), Sea salt injections into the low-latitude marine boundary layer: The transient response in three Earth System Models, *J. Geophys. Res. Atmos.*, *118*, 12,195–12,206.

Bala, G., and B. Nag (2011), Albedo enhancement over land to counteract global warming: Impacts on hydrological cycle, *Clim. Dyn.*, *37*, doi:10.1007/s00382-011-1256-1.

Bala, G., P. B. Duffy, and K. E. Taylor (2008), Impact of geoengineering schemes on the global hydrological cycle, *Proc. Natl. Acad. Sci. U.S.A.*, *105*, 7664–7669.

Bala, G., K. Caldeira, and R. Nemani (2010), Fast versus slow response in climate change: Implications for the global hydrological cycle, *Clim. Dyn.*, *35*, 423–434, doi:10.1007/s00382-009-0583-y.

Bala, G., K. Caldeira, R. Nemani, L. Cao, G. Ban-Weiss, and H.-J. Shin (2011), Albedo enhancement of marine clouds to counteract global warming: Impacts on the hydrological cycle, *Clim. Dyn.*, *37*, 915–931, doi:10.1007/s00382-010-0868-1.

Bentsen, M., et al. (2013), The Norwegian Earth System Model, NorESM1-M—Part 1: Description and basic evaluation of the physical climate, *Geosci. Model Dev.*, *6*, 687–720, doi:10.5194/gmd-6-687-2013.

Bleck, R., C. Rooth, D. Hu, and L. T. Smith (1992), Salinity-driven thermocline transients in a wind- and thermohaline-forced isopycnic coordinate model of the North Atlantic, *J. Phys. Oceanogr.*, *22*, 1486–1505.

Collins, M., et al. (2013), Long-term climate change: Projections, commitments and irreversibility, in *Climate Change 2013: The Physical Science Basis. Contribution of Working Group I to the Fifth Assessment Report of the Intergovernmental Panel on Climate Change*, edited by T. F. Stocker et al., pp. 1029–1136, Cambridge Univ. Press, Cambridge, U. K., and New York, doi:10.1017/CBO9781107415324.024.

Crutzen, P. (2006), Albedo enhancement by stratospheric sulfur injections: A contribution to resolve a policy dilemma?—An Editorial Essay, *Clim. Change*, *77*, 211–219.

Feichter, J., E. Rockner, U. Lohmann, and B. Liepert (2004), Nonlinear aspects of the climate response to greenhouse gas and aerosol forcing, *J. Clim.*, *17*, 2384–2398.

Feng, S., and Q. Fu (2013), Expansion of global drylands under a warming climate, *Atmos. Chem. Phys.*, *13*, 10,081–10,094.

Haywood, J. M., A. Jones, N. Bellouin, and D. Stephenson (2013), Asymmetric forcing frmo stratospheric aerosols impacts Sahelian rainfall, *Nat. Clim. Change*, *3*, 660–665.

Held, I. M., and B. J. Soden (2006), Robust responses of the hydrological cycle to global warming, *J. Clim.*, *19*, 5686–5699, doi:10.1175/JCLI3990.1.

Hoose, C., J. E. Kristjánsson, T. Iversen, A. Kirkevåg, Ø. Seland, and A. Gettelman (2009), Constraining cloud droplet number concentration in GCMs suppresses the aerosol indirect effect, *Geophys. Res. Lett.*, *36*, L12807, doi:10.1029/2009GL038568.

Irvine, P. J., A. Ridgwell, and D. J. Lunt (2010), Assessing the regional disparities in geoengineering impacts, *Geophys. Res. Lett.*, *37*, L18702, doi:10.1029/2010GL044447.

Kirkevåg, A., et al. (2013), Aerosol–climate interactions in the Norwegian Earth System Model—NorESM1-M, *Geosci. Model Dev.*, *6*, 207–244, doi:10.5194/gmd-6-207-2013.

Kleidon, A., B. Kravitz, and M. Renner (2015), The hydrological sensitivity to global warming and solar geoengineering derived from thermodynamic constraints, *Geophys. Res. Lett.*, *42*, 138–144, doi:10.1002/2014GL062589.

Kravitz, B., A. Robock, O. Boucher, H. Schmidt, K. E. Taylor, G. Stenchikov, and M. Schulz (2011), The Geoengineering Model Intercomparison Project (GeoMIP), *Atmos. Sci. Lett.*, *12*(2), 162–167, doi:10.1002/asl.316.

Kravitz, B., et al. (2013a), Climate model response from the Geoengineering Model Intercomparison Project (GeoMIP), *J. Geophys. Res. Atmos.*, *118*, 8320–8332, doi:10.1002/jgrd.50646.

Kravitz, B., et al. (2013b), An energetic perspective on hydrological cycle changes in the Geoengineering Model Intercomparison Project (GeoMIP), *J. Geophys. Res. Atmos.*, *118*, 13,087–13,102, doi:10.1002/2013JD020502.

Kravitz, B., et al. (2015), The Geoengineering Model Intercomparison Project Phase 6 (GeoMIP6): Simulation design and preliminary results, *Geosci. Model Dev. Discuss.*, *8*, 4697–4736, doi:10.5194/gmdd-8-4697-2015.

Lawrence, D. M., et al. (2011), Parameterization improvements and functional and structural advances in version 4 of the Community Land Model, *J. Adv. Model. Earth Sys.*, *3*, doi:10.1029/2011MS000045.

McVicar, T. R., L. Li, T. G. Van Niel, M. F. Hutchinson, X. Mu, and Z. Liu (2005), Spatially distributing 21 years of monthly hydrometeorological data in China: Spatio-temporal analysis of FAO-56 Crop Reference Evapotranspiration and Pan Evaporation in the context of climate change. CSIRO Land and Water Tech. Rep. 8/05, 324 pp.

Mitchell, D. L., and W. Finnegan (2009), Modification of cirrus clouds to reduce global warming, *Environ. Res. Lett.*, *4*(4, 045102), doi:10.1088/1748-9326/4/4/045102.

Mitchell, J. F. B., C. A. Wilson, and W. M. Cunnington (1987), On CO_2 climate sensitivity and model dependence of results, *Q. J. R. Meteorol. Soc.*, *113*, 293–322.

Muri, H., J. E. Kristjánsson, T. Storelvmo, and M. A. Pfeffer (2014), The climatic effects of modifying cirrus clouds in a climate engineering framework, *J. Geophys. Res. Atmos.*, *119*, 4174–4191, doi:10.1002/2013JD021063.

Neale, R. B., et al. (2010), Description of the NCAR Community Atmosphere Model (CAM 4.0), Tech. Rep. *NCAR/TN-485+STR*, Natl. Center for Atmos. Res., 212 pp., Boulder, Colo.

Niemeier, U., H. Schmidt, K. Alterskjær, and J. E. Kristjánsson (2013), Solar irradiance reduction via climate engineering —Climatic impact of different techniques, *J. Geophys. Res. Atmos.*, *118*, 11,905–11,917, doi:10.1002/2013JD020445.

Oleson, K. W., et al. (2010), Technical description of version 4.0 of the Community Land Model (CLM), *NCAR/TN-478+STR*, Natl. Center for Atmos. Res., Boulder, Colo., 257 pp.

Robock, A., L. Oman, and G. L. Stenchikov (2008), Regional climate responses to geoengineering with tropical and Arctic SO_2 injections, *J. Geophys. Res.*, *113*, D16101, doi:10.1029/2008JD010050.

Schäfer, S., M. Lawrence, H. Stelzer, W. Born, and S. Low (Eds.) (2015), *The European Transdisciplinary Assessment of Climate Engineering (EuTRACE), Final Rep. of the FP7 CSA Project EuTRACE*, 170 pp. Institute for Advanced Sustainability Studies (IASS), Potsdam, Germany.

Schmidt, H., et al. (2012), Solar irradiance reduction to counteract radiative forcing from a quadrupling of CO_2: Climate response simulated by four Earth system models, *Earth Syst. Dyn.*, *3*, 63–78.

Sherwood, S., and Q. Fu (2014), A drier future?, *Science*, *343*, 737–739.

Storelvmo, T., and N. Herger (2014), Cirrus cloud susceptibility to the injection of ice nuclei in the upper troposphere, *J. Geophys. Res. Atmos.*, *119*, 2375–2389.

Storelvmo, T., J. E. Kristjánsson, H. Muri, M. Pfeffer, D. Barahona, and A. Nenes (2013), Cirrus cloud seeding has potential to cool climate, *Geophys. Res. Lett.*, *40*, 178–182, doi:10.1029/2012GL054201.

Storelvmo, T., W. Boos, and N. Herger (2014), Cirrus cloud seeding—A climate engineering mechanism with reduced side effects?, *Phil. Trans. R. Soc., A*, *372*, doi:10.1098/rsta.2014.0116.

Syed, T. H., J. S. Famiglietti, D. P. Chambers, J. K. Willise, and K. Hilburn (2010), Satellite-based global-ocean mass balance estimates of interannual variability and emerging trends in continental freshwater discharge, *Proc. Natl. Acad. Sci. U.S.A.*, *107*, 17,916–17,921.

Tilmes, S., et al. (2013), The hydrological impact of geoengineering in the Geoengineering Model Intercomparison Project (GeoMIP), *J. Geophys. Res. Atmos.*, *118*, 11,036–11,058, doi:10.1002/jgrd.50868.

Trenberth, K. E., J. M. Caron, and D. P. Stepaniak (2001), The atmospheric energy budget and implications for surface fluxes and ocean heat transports, *Clim. Dyn.*, *17*, 259–276.

Wu, P., R. Wood, J. Ridley, and J. Lowe (2010), Temporary acceleration of the hydrological cycle in response to a CO_2 rampdown, *Geophys. Res. Lett.*, *37*, L12705, doi:10.1029/2010GL043730.